ELSEVIER

Journal of Power Sources 81–82 (1999) 286–290

JOURNAL OF POWER SOURCES

www.elsevier.com/locate/jpowsour

Temperature dependence of the passivation layer on graphite

A.M. Andersson [a,*], K. Edström [a], N. Rao [b], Å. Wendsjö [b]

[a] *Inorganic Chemistry, Ångström Laboratory, Uppsala University, Box 538, SE-751 21 Uppsala, Sweden*
[b] *Danionics, Hestehaven 21J, DK-5260 Odense S, Denmark*

Abstract

The elevated temperature stability of the Solid Electrolyte Interface (SEI) formed on graphite during the first charge/discharge cycle has been investigated. This was done in order to determine its role in the high-temperature degradation process which occurs in a $C/LiMn_2O_4$ Li-ion cell. X-ray photoelectron spectroscopy (XPS) is used to probe the surface-layer growth and elemental composition of graphite electrodes exposed to different thermal treatment. The surfaces of cycled electrodes, when stored below 60°C, were seen to resemble closely those of unstored electrodes. An electrode stored at 60°C exhibited a significant increase in the amount of oxidized carbon and oxygen. Analysis by Ar sputtering suggests that a thick 'macroscopic' layer coats the graphite electrode surface, but not the separate graphite grains; this is consistent with the observed rapid decrease in capacity and large cell-resistance on cycling such cells after storage. This capacity decrease was not observed for the cells stored at RT and 40°C.

Keywords: Li-ion batteries; Graphite anode; High-temperature performance; X-ray photoelectron spectroscopy

1. Introduction

Ambient and elevated temperature stability is a crucial factor in the performance of batteries for the ever-growing portable electronics market. Poor performance and premature 'cell death' have been reported for $C/LiMn_2O_4$ Li-ion cells exposed to temperatures above 55°C [1]. Several groups have reported various parasitic reactions occurring at the cathode. Typically, oxidation of the electrolyte occurs at the spinel surface when the cell is charged and the open circuit potential is high [2]. Moreover, these reactions are more aggressive at elevated temperatures. Manganese dissolution reactions also threaten high-temperature cathode stability; the spinel electrode is corroded by traces of HF in the electrolyte, and Mn^{2+} ions are transferred to the electrolyte [1]. Although such cathode-related reactions tend to be seen as the major contributor to high-temperature cell failure, the carbon electrode is also known to be unstable at these temperatures. In a charged cell, with Li^+ ions intercalated into the carbon, the Li_xC phases and the electrolyte are believed to undergo an exothermic reaction at elevated temperatures, leading to delithiation of the carbon and the formation of an additional solid electrolyte interface (SEI) layer on top of that already formed on the carbon surface, with resulting loss of capacity [3,4]. However, the extent to which these reactions occur, and how they are related to the salts and solvents used in the electrolyte, have so far not been fully investigated. The destruction of the SEI layer in the discharged state, brought about by temperature induced reactions between the SEI and electrolyte species, has been discussed in earlier publications, but has not been analysed completely [4].

The use of graphitic carbon as active anode material in Li-ion cells provides for a high energy density and good cycling performance. While the formation of the SEI layer on the graphite particles during the first charging (intercalation) of the cell brings with it certain disadvantages (irreversible capacity loss), provided that the film remains thin and covers the entire graphite surface, it preserves the favourable electrochemical properties of the graphite. The composition, functionality and morphology of the SEI layer is determined by the salts and solvents used in the electrolyte. The film formed on the graphite grains during the first charge, using $LiBF_4$ salt in the standard EC/DMC alkyl carbonate liquid electrolyte, is known to contain some electrolyte–solvent reaction products such as Li_2CO_3 and CH_3CO_3Li, and additional salt and trace–water reduction products, mainly LiF, as determined by FTIR spectroscopy [5]. While this technique provides qualitative information about the nature of the surface, X-ray Photo-

* Corresponding author. Tel.: +44-18-471-37-37; Fax: +44-18-51-35-48; E-mail: ami@kemi.uu.se.

0378-7753/99/$ - see front matter
PII: S0378-7753(99)00202-5

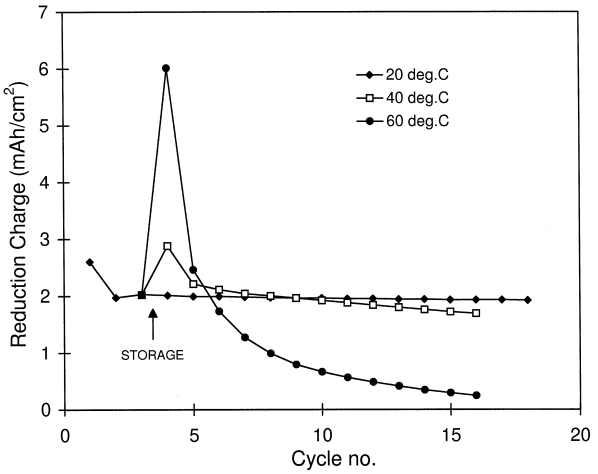

Fig. 1. Reduction charge vs. cycle number for Li/graphite half-cells precycled three times at room temperature (cycle nos. 1–3) prior to storage at different temperatures for 7 days, followed by continued cycling at these same temperatures.

electron Spectroscopy provides a quantitative analysis of the surface composition and surface-layer thickness [6]. These features have been exploited here, where the main goal has been to analyse specifically the stability of the SEI layer on graphite at elevated temperatures. This has been done for standard Li/C half-cells, using the standard electrolyte referred to above, as a model system. Graphite electrodes are analysed in their discharged (deintercalated) state, so that the reactions which relate solely to the SEI layer can be focused upon, without interference from other temperature related reactions at the anode or cathode, such as delithiation or Mn dissolution related reactions.

2. Experimental

2.1. Half-cell preparation

Carbon electrodes were typically prepared by spreading a mix of 90 wt.% Timrex KS6 graphite (Timcal, Switzerland), 5 wt.% Shewinigan Black carbon powder and 5 wt.% EPDM rubber binder in cyclohexane onto a porous Ni-foil current collector (Fukuda Metal Foil and Powder, Japan). The graphite loading on the current collector was typically 5.4 mg/cm^2. The electrodes were cut into 7 or 25 cm^2 pieces and dried under vacuum at 120°C, before laminating them with a glass-wool separator soaked in electrolyte and the Li-foil counter electrode. A Li reference electrode was also placed in the battery stack to facilitate three-electrode studies. The laminates were packed in polymer-coated aluminium bags, evacuated and sealed. The electrolyte used in all experiments was 1 M $LiBF_4$ (Tomiyama) in EC/DMC (2:1) (Selectipur®, Merck, Darmstadt, Germany). The salt was dried in vacuum at 120°C prior to use, and the solvents were used *as received*. The cells were assembled and packed in an argon-filled glove-box (< 3 ppm H_2O and O_2).

2.2. Electrochemical measurements

All cell-cycling experiments were conducted at C/2 rate. The three-electrode set-up was used to follow exclusively the potential changes of the graphite electrode. Equivalent cells were precycled three times between 10 mV and 1.5 V, with a relaxation period of 10 min at the end of each discharge/charge. The cycling procedure was interrupted at the 1.5 V cut-off voltage, i.e., with the graphite electrodes in their deintercalated state.

The SEI layer formed during these initial cycles is generally seen as a thin, uniform film which provides a perfect passivation layer for the graphite grains. The chemical features of this film were analysed by DSC and XPS (see below). The precycling of a number of equivalent cells was followed by storing the cells at 20°C (RT), 40°C or 60°C for 7 days, to allow any reactions occurring at these temperatures to reach completion. Three of these stored electrodes were then also analysed with XPS, while the remainder of the cells continued to cycle at C/2 rate at the same temperatures at which they had been stored. The resistance of the cells was measured during the relaxation period at the end of each discharge while the current was declining toward zero.

2.3. DSC measurements

The precycled, vacuum-sealed cells were dismantled in an Ar filled glove-box, and the electrodes were cut into small pieces (5.20 mg of active material), and sealed in standard Al crucibles. The measurements were carried out on a Mettler DSC 30 calorimeter, with the heating rate set at 5°C/min in the temperature range 20°C to 400°C. Complementary measurements were made on the 'pure' materials used in the cells, e.g., Li metal foil, Li-salts, solvents, graphite powder, Ni-foil current collector and EPDM binder, and mixtures thereof.

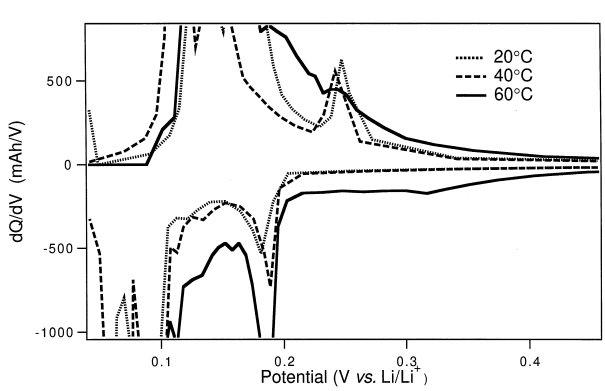

Fig. 2. Plots of dQ/dV vs. potential during the first cycle for cells stored at different temperatures. The cycling is conducted at the same temperatures as the storage.

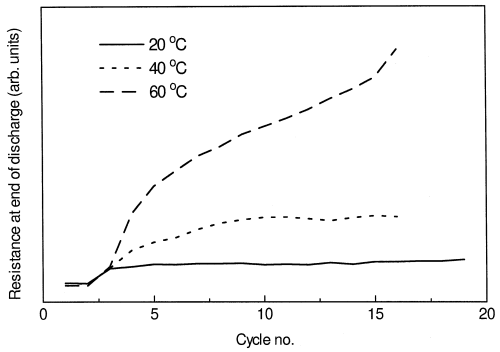

Fig. 3. Resistance at the end of discharge plotted as a function of cycle number and storage temperature.

2.4. XPS measurements

The XPS measurements were conducted on a PHI 5500 system, using an Al Kα excitation source. The cells which had been exposed to the various pre-treatments were cut open in the glove-box and small pieces of the graphite electrodes were mounted on XPS sample holders. The holders were then vacuum-sealed in a polymer laminated aluminium bag in the glove-box, and transported to the XPS apparatus where they were cut open and placed in the spectrometer introduction chamber under a flow of N_2 (g). The samples were first analysed as prepared, and then sputtered with an Ar beam until the amounts of the different elements reached a 'steady state' at which the surface layer of the topmost graphite grains had been sputtered off. They were then reanalysed.

All cycling and XPS studies were performed twice; essentially the same results were obtained.

3. Results

3.1. Electrochemical cycling

The total reduction charge of the different cells have been extracted from the cycling data and plotted vs. number of cycles; the results are shown in Fig. 1.

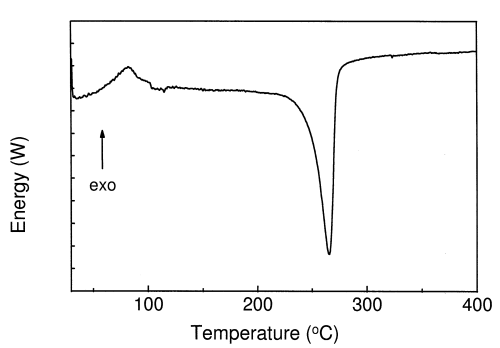

Fig. 4. DSC trace of a deintercalated graphite electrode (no storage).

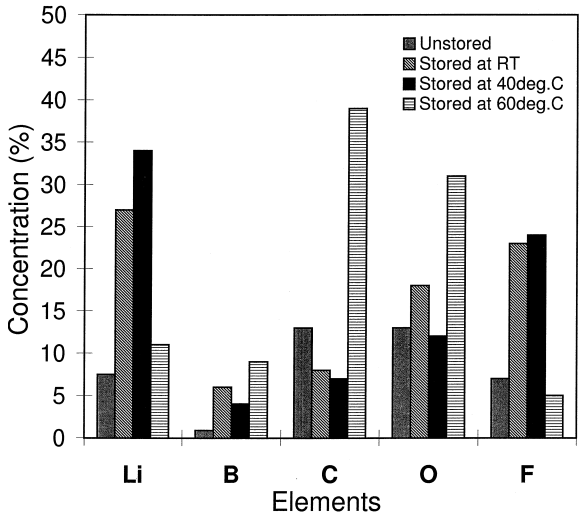

Fig. 5. Elemental analysis of the graphite electrode surface; $LiBF_4$ and graphite contribution is subtracted.

The increased intercalation capacities in cycle 4 for the samples stored above room temperature suggest secondary redox reactions occurring in the cell. dQ/dV plots for cycle 4 reveal no additional solvent reduction around 0.7 V as in the formation of the original SEI film; there is, however, an additional reduction peak at 0.3 V for the cell stored at 60°C (Fig. 2).

The cells stored at RT and 40°C could be cycled continuously from cycle 5 onward with only small losses in capacity. The cells stored at 60°C, however, showed a continuous loss in capacity, leading to 'cell death' within 10 cycles. The resistance of the heat-treated cells clearly increases after storage, becoming more than 3 times larger for the '60°C cell' on continued cycling (Fig. 3).

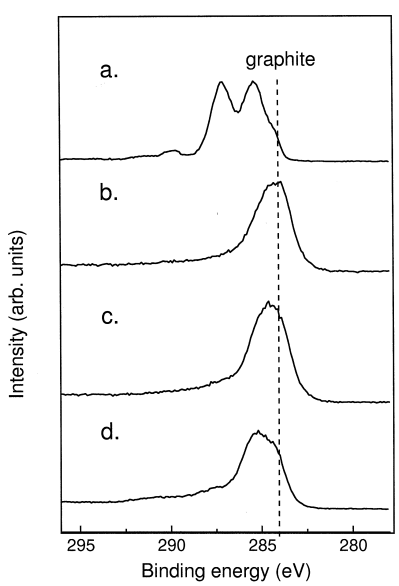

Fig. 6. The influence of storage temperature on the C1s XPS spectrum of graphite electrodes; (a) storage at 60°C, (b) 40°C, (c) 20°C, (d) unstored electrode.

Spinel cathode half-cells treated in the same way as above display neither the increased reduction charge during cycle 4, nor the large drop in capacity on continued cycling. The elevated temperature performance of the graphite half-cells is thus not a result of poor Li-electrode performance, but reflects graphite electrode and electrolyte effects alone.

3.2. DSC results

Fig. 4 shows the DSC trace for a deintercalated graphite electrode after cycles 1–3. Two features can be observed: the large endothermic peak assigned to chemical reactions involving the electrolyte solution, and the exothermic peak with its maximum at 79.5°C which can be assigned to a reaction involving the SEI layer.

3.3. XPS results

The elements detected on the surface of the graphite electrodes were, in all cases: F, O, C, B and Li, where certain peak shifts could be assigned directly to the $LiBF_4$ salt, LiF and graphite. The amount of each element was calculated by integrating the intensities of the XPS peaks and correcting for the cross-section for the ionisation of each element. The contribution from $LiBF_4$ and graphite were subtracted in the elemental analysis of the surface layer. The relative concentrations of the different elements found on the surface of the stored and unstored samples are shown in Fig. 5. An increase in Li and F content occurs on storing the samples at RT and 40°C. The shifts in the Li and F peaks were assigned to the formation of LiF.

The C and O content on the surface increased significantly for the sample stored at 60°C (Fig. 5). The C1s XPS peak shifts (Fig. 6) clearly show the evolution of C, with higher oxidation state on the surface of the '60°C electrode'. The C and O increase is coupled to a decrease in Li and F content. Fig. 7 shows the relative concentrations of the elements on the graphite surface after Ar sputtering. It is clear that, when the outer layer of the electrode had been removed by sputtering, the electrodes had a very similar composition. A compositional 'steady state' was reached for the electrodes stored at RT and 40°C after less than 40 s sputtering; however, it took more than 10 min to arrive at a constant C concentration for the electrode stored at 60°C.

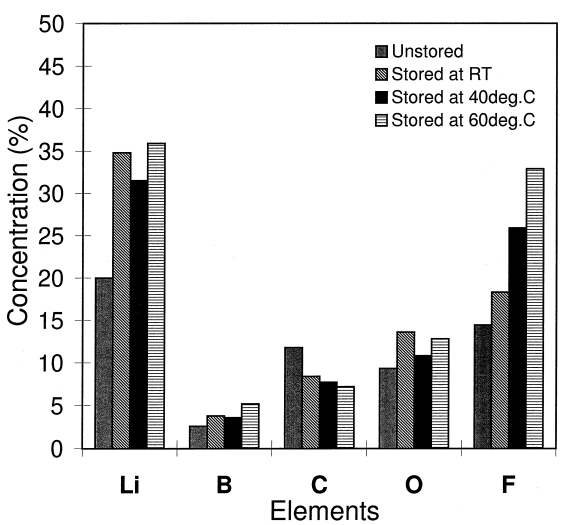

Fig. 7. Elemental analysis of the graphite electrode surface after Ar sputtering until a compositional 'steady state' is reached; $LiBF_4$ and graphite contribution subtracted.

4. Discussion

From the above, the surface species on the graphite electrode are clearly seen to be influenced by elevated temperature. Evidence of several types of contributing reaction can be distinguished in the measurements.

The XPS measurements indicate that storing the cells caused an increase in LiF content on the graphite electrode surfaces (Fig. 5); presumably a product of the acid–base reaction suggested by Kanamura et al. [6]:

$$LiBF_4 + H_2O \rightarrow 2HF + LiF + BOF \quad (1)$$

This reaction can occur both on the graphite surface and in the bulk electrolyte; the precipitation of LiF is, therefore, not limited to the surface. Aurbach et al. have proposed [5] the conversion of Li_2CO_3 on the graphite surface to LiF according to:

$$Li_2CO_3 + 2HF \rightarrow 2LiF + H_2CO_3 \quad (2)$$

This type of reaction is typical for $LiPF_6$- and $LiBF_4$-containing electrolytes, but is claimed to be more pronounced in the latter case. However, the LiF layer covering the graphite grains seems to remain sufficiently thin or porous to allow reasonable transport of the Li^+ ions during the continued cycling, even up to 40°C. The graphite shift in the C peak (at 284.2 eV) for the '20°C electrode' and '40°C electrode' is still clearly observable after storage (Fig. 6), which again suggests only small changes in the thickness of the surface layer. The relatively large amount of LiF formed on the graphite surface would seem to precipitate from the electrolyte (Eq. (1)) to form small clusters within the electrode, leaving most of the graphite surface available for Li^+-ion penetration.

Cells stored at 60°C experience more severe damage to the graphite electrode surface. The XPS results clearly show that an additional surface layer is formed during the storage. The elemental composition of all stored electrodes was very similar, however, after Ar sputtering, which would indicate that the secondary layer on the 60°C sample, is formed 'macroscopically' on the electrode surface, and does not surround each individual graphite grain, as does the SEI layer (Fig. 8).

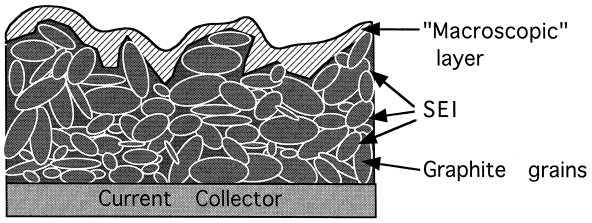

Fig. 8. A schematic representation of a graphite electrode stored at 60°C for 7 days.

The roughness of the electrodes means that it is difficult to estimate the actual thickness of the surface layers on the graphite. The mosaicity of species that build up the different layers also implies that it is difficult to relate sputtering time and sputtering depth. XPS measurements on reference samples with known surface-layer thickness are needed. It is clear from Fig. 6, however, that the intensity of the graphite shift in the '60°C electrode' has decreased significantly as the surface layer has grown. The thicker layer can function as a shield which effectively hinders the Li^+ ions from penetrating through to the active electrode. The XPS result is consistent with the electrochemical cycling experiments, which also indicate a blocking of the electrode and accompanying capacity fade for the '60°C cell'.

Additional redox reactions during cycle 4, resulting in the irreversible capacity loss, may also have implications for the subsequent cycling performance. These reactions can arise from a number of sources, e.g., exposure of the graphite surface through the dissolution of the passivation layer (Li carbonates, etc.), changes in the graphite surface structure (e.g., exfoliation) and the subsequent formation of a second SEI layer. Further studies are needed, however, to better understand the origins of this process.

5. Conclusions

The surface chemistry of a graphite anode in conjunction with an electrolyte containing $LiBF_4$ is clearly affected by treatment at elevated temperature. Galvanostatic cycling in conjunction with XPS has been used here in a novel way to characterise electrochemical performance, surface composition and passivation layer growth on graphite electrodes cycled and stored in their deintercalated state.

The XPS measurements are compatible with a model assuming an additional passivation layer on the 'macroscopic' surface of the graphite electrode for Li/C half-cells stored at 60°C. The thickness of this new layer far exceeds that of the original SEI layer, even if this cannot be quantified at this stage. An increase in cell resistance and a related rapidly declining capacity is observed for these cells; this is consistent with the creation of an additional surface layer. Storing the cells also causes an increase in the amount of LiF on the surface of the electrodes at all temperatures.

Acknowledgements

This work has been supported by the EU (Joule III) Programme, and in Sweden by The Swedish Natural Science Research Council (NFR) and The Board for Technical Development (NUTEK) within projects led by Prof. Josh Thomas.

References

[1] G.G. Amatucci, C.N. Schmutz, A. Blyr, C. Sigala, A.S. Gozdz, D. Larcher, J.M. Tarascon, J. Power Sources 69 (1997) 11.
[2] D.H. Jang, Y.J. Shin, S.M. Oh, J. Electrochem. Soc. 143 (1996) 2204.
[3] U. von Sacken, E. Nodwell, A. Sundher, J.R. Dahn, J. Power Sources 54 (1995) 240.
[4] A. Blyr, C. Sigala, G. Amatucci, D. Guyomard, Y. Chabre, J.M. Tarascon, J. Electrochem. Soc. 145 (1998) 194.
[5] D. Aurbach, Y. Ein-Eli, B. Markovsky, A. Zaban, S. Luski, Y. Carmeli, H. Yamin, J. Electrochem. Soc. 142 (1995) 2882.
[6] K. Kanamura, H. Tamura, S. Shiraishi, Z. Takehara, J. Electrochem. Soc. 142 (1995) 340.